

# **Egyptian Journal of Chemistry**

http://ejchem.journals.ekb.eg/



Novel organophosphonates based on the pyrazole moiety as potent antimicrobial agents: synthesis, characterization, molecular docking studies, and DFT calculations

Mansoura A. Abd-El-Maksoud<sup>a</sup>, Basma Ghazal<sup>a</sup>, Mohamed S. Abdel-Aziz<sup>b</sup>, Marwa El-Hussieny<sup>a\*</sup>

"Organometallic and Organometalloid Chemistry Department, Chemical Industries Research Institute, National
Research Centre, 33 El Behouth St., Dokki P.O. 12622, Giza, Egypt.

<sup>b</sup>Microbial Chemistry Department, Genatic Engineering and Biotechnology Institute, National Research Centre, 33 E lBohouth St., Dokki P.O. 12622, Giza, Egypt

#### Abstract

In the present study, trimethoxy-oxaphosphol-pyrazol-3-one and dimethyl-pyrazoloxobutylphosphonate derivatives were produced when chalcones incorporated pyrazolone ring 1a,b interacted with trimethyl phosphite in a free solvent setting with palladium acetate acting as a catalyst. However using dialkyl phosphites resulted in a phosphonate derivative. Moreover, organophosphonte derivatives have been prepared via the reaction of pyrazole substrates and dialkyl phosphites. On the other hand, bis(dimethylamino) phosphorylpropanoyl methane and bis(dimethylamino) phosphorylpropanoyl benzene were prepared through the reaction of 5-pyrazolones with hexamethylphosphinetriamine. Spectroscopic analysis was performed to confirm the structure of all new compounds. The in-vitro antibacterial and antifungal activities for all new synthesized compounds were carried out. The obtained results are compared with the reference antibiotics namely, Neomycin (bactericide) and Cyclohexamide (fungicide). Additionally, all of the substances under study showed good to moderate activity compared to the standards, according to the Minimum Inhibitory Concentration (MIC) measurements. The geometry of the compounds was adjusted using density function theory (DFT) at B3LYP using 6-311 G (d,p) basis in order to investigate the electronic characteristics and reactivity of all the compounds under study. Additionally, by inhibiting Dihydropteroate synthase, the molecular docking methodology shows the antibacterial activity of the created compounds, and all of the designed compounds have demonstrated notable drug-like properties.

**Keywords.** Chalcones; oxaphosphole; molecular docking; DFT; antimicrobial agents; MIC.

# 1- Introduction:

Phosphonate derivatives represent an important and versatile class of organophosphorus compounds with wideranging biological applications, particularly in medicinal chemistry. Their distinctive chemical features, such as the presence of a stable C–P bond and the ability to mimic biological phosphate esters [1], make them attractive scaffolds for the development of new antimicrobial agents [2-5]. The incorporation of phosphonate functionalities into organic frameworks can significantly enhance lipophilicity, improve metabolic stability, and modulate biological activity [6, 7]. Figure 1 showed some of active phosphonate drugs.

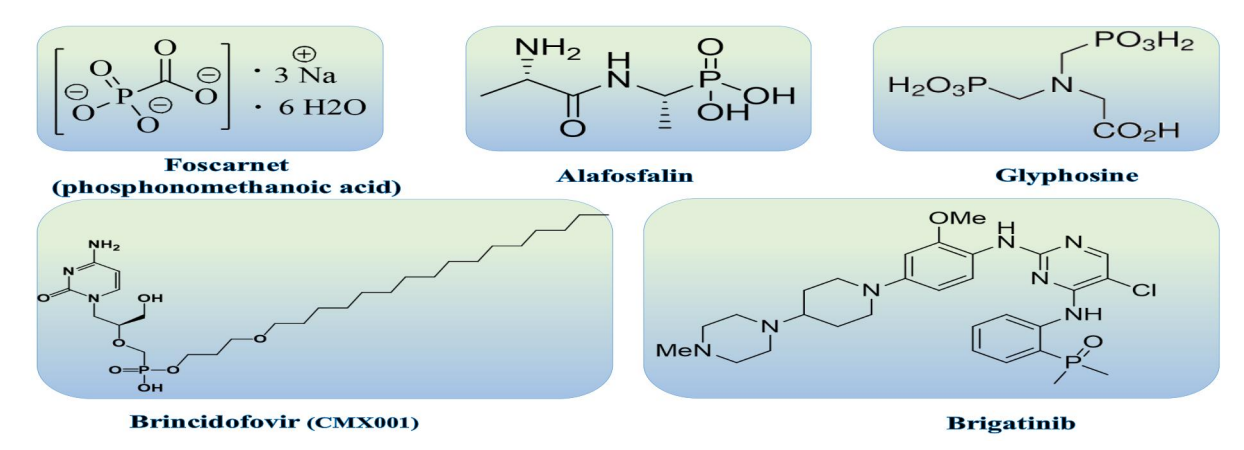


Figure 1: Structures of biologically active phosphonate drugs.

\*Corresponding author e-mail: mrw\_elhussieny@yahoo.com.; (Marwa El-Hussieny). Received Date: 18 July 2025, Revised Date: 29 August 2025, Accepted Date: 01 September 2025 DOI: 10.21608/EJCHEM.2025.405317.12064

©2026 National Information and Documentation Center (NIDOC)

Within this domain, chalcone-based frameworks have drawn considerable attention due to their remarkable pharmacological versatility. Chalcones, characterized by the  $\alpha$ , $\beta$ -unsaturated carbonyl system, exhibit diverse biological activities, including antibacterial, antifungal, anti-inflammatory, and anticancer properties [8-10]. The conjugation of chalcone skeletons with heterocycles such as pyrazole has been reported to further improve their potency and selectivity [11, 12]. Pyrazole-containing chalcones benefit from the synergistic combination of two bioactive motifs: the pyrazole nucleus, known for its antimicrobial, anti-tubercular, and anti-parasitic activities [13, 14], and the chalcone moiety, which can disrupt microbial enzymatic systems and membrane functions [15, 16].

Previous studies have demonstrated that structural modifications, such as the introduction of phosphonate groups into chalcone–pyrazole hybrids, can lead to novel molecular entities with enhanced antimicrobial properties . This is attributed to the dual mechanism: (i) the electrophilic chalcone α,β-unsaturated carbonyl group, capable of interacting with nucleophilic residues in microbial enzymes, and (ii) the phosphonate group, which can mimic natural phosphate substrates and interfere with microbial metabolic pathways [17]. Given the rising threat of antimicrobial resistance, the design and synthesis of such hybrid molecules represent a promising strategy in drug discovery. Therefore, the present study focuses on the synthesis of novel chalcone derivatives containing pyrazole rings functionalized with phosphonate groups. The antimicrobial activities of the synthesized compounds will be evaluated against selected Gram-positive and Gram-negative bacterial strains, as well as pathogenic fungi, with their efficacy compared to established reference antibiotics. According to many applications of organophosphorus compounds as phosphorus-based organocatalysis and its applications in medicinal chemistry, production of phosphonates of pharmaceutical purposes. Density functional theory had been used to simulate the electronic properties of novel compounds. Frontier molecular orbitals, NBO, dipole moments and different electronic descriptors were all inspected through computational investigation. In addition to validate the DFT pharmacokinetics and molecular docking study.

# 2- Results and Discussion

# 2.1. Chemistry

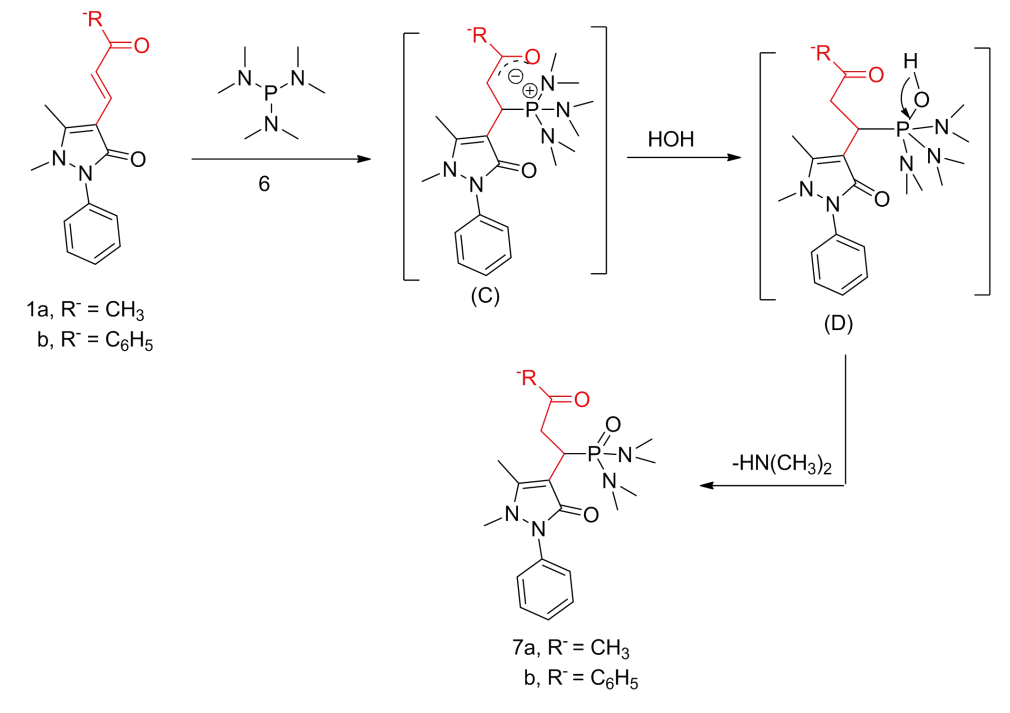
Reactions of α,β-unsaturated carbonyl compounds with different organophosphorus reagents were studied previously to prepare bioactive compounds for pharmaceutical purposes [18-25]. Moreover, oxobutenylpyrazolone and oxophenylpropenylpyrazolone with alkylphosphites are also discussed for synthesizing chalcone precursors containing phosphonate moiety and screening their antimicrobial activities. Therefore, when 1,5-dimethyl-4-(3-oxobut-1-en-1-yl)-2-phenyl-1H-pyrazol-3(2H)-one (1a) reacts with trimethyl phosphite (2a) without solvent in the presence of palladium acetate as a catalyst gave two products 3a and 4a. The reaction proceeded *via* nucleophilic attack by 2a on both carbonyl-C and double C=C of chalcone 1a to form the intermediate dipolar adduct (A) which undergoes ring closure affords phospholane derivative 3a [26, 27]. Due to unavoidable moisture the intermediate (A) can be hydrolyzed to form dialkyl phosphonate derivative 4a through the extrusion of alcohol molecule. Besides, when oxophenylpropenylpyrazolone 1a was reacted with TAP gave 3b and 4b (scheme 1). The chemical structures of 3a and 4a were assured using microanalyses and several spectroscopic data.

On the other side, when two  $\alpha$ ,  $\beta$ -unsaturated compounds 1a and 1b reacted with triisopropylphosphite (TIP, 2b) gave the corresponding 4b and 4f respectively. Moreover, the reaction of dialkylphosphites (5a-c) and chalcones (1a,b) is also studied. When chalcones (1a,b) reacted with dimethyl- (5a), diethyl- (5b) and diisopropylphosphite (5c), the corresponding phosphonate derivatives (4a-f) were performed (scheme 1). Furthermore, hexamethylphosphinetriamine (6) was permitted to react with 1a,b resulting in the unequivocally formation of 7a,b, respectively (scheme 2). The phosphonates derivatives 7a,b were formed through phosphorus

atom of the aminophosphine **6** on the most interacting center, the methine carbon of starting materials **1a,b** which results in the formation of the dipolar adduct (C). While the addition of a water molecule (atmospheric moisture) to the intermediate (C) that producing intermediate (D) leads to form final products **7a,b** *via* HN(CH<sub>3</sub>)<sub>2</sub> molecule was expelled.

molecule was expelled.

Scheme 1. Synthesis of dialkyl phosphonate derivatives 3(a,b), 4(a-f) and 5(a-c).



Scheme 2. Synthesis of dialkyl phosphonate 7(a,b).

# 2.2 Biological Evaluation

#### **Antimicrobial activity**

**Table 1.** The antimicrobial activity of the new compounds against different tests.

							Inl	hibiti	on Cl	ear Z	one (	(mm)			
	Gram Stain Reaction		F									eference tibiotics			
Microorganism		1a	1b	3a	3b	4a	4b	4c	4d	4e	4f	7a	7b	Neomycin	Cycloheximide
Staphylococcus aureus	Positive	0	12	0	13	0	0	24	17	19	20	19	17	29	0
Escherichia coli	Negative	15	12	0	0	0	0	28	0	23	24	0	17	26	0
Candida albicans	Yeast	0	0	0	0	0	0	29	13	21	19	15	18	27	0
Aspergillus niger	Fungus	15	14	14	17	15	0	23	0	0	14	13	0	0	30

In most developing countries, pathogenic bacteria are responsible for the main causes of hazards to public health. Therefore, Starting 5-pyrazolones 1a, 1b and all newly synthesized compounds 3a, 3b, 4a, 4b, 4c, 4d, 4e, 4f, 7a and 7b were assessed for antibacterial activities *in vitro* against *Staphylococcus aureus* ATCC 6538-P as G+ve bacteria, *Escherichia coli* ATCC 25933 as G-ve bacteria, *Candida albicans* ATCC 10231 as yeast and *Aspergillus niger* NRRL as filamentous fungus test microbe using cup agar diffusion method in comparison to Neomycin as anti-bacterial drug and cycloheximide as anti-fungal drug and the minimum inhibitory concentrations (MIC) for the more active compounds (4c-f) and 7b were determined, too.

Table 2. Minimum inhibition concentration (MIC) of 4c-f and 7b against different test microbes

Sample	Staphylococcus aureus MIC (μg/ml)	Escherichia coli MIC (μg/ml)	<i>Candida albicans</i> MIC (μg/ml)
4c	312.5	156.25	78.12
<b>4e</b>	312.5	78.12	156.25
<b>4f</b>	156.25	156.25	156.25
<b>7b</b>	156.25	156.25	78.12

As shown in Table 1 and 2, the anti-bacterial results showed that all of the tested compounds had moderate to good efficacy against G+ve and G-ve of the pathogenic bacteria and they also showed their inhibition zones. Compound 4c is potent for *Escherichia coli* with MIC 78.12 (μg/ml) [28, 29] which has activity closely related the two reference antibiotics (Neomycin and cycloheximide) and the other compounds (4e, 4f and 7b) had a moderate effect with MIC, 156.25 (μg/ml). In case of *Staphylococcus aureus* pathogen, the results of the MIC of these compounds (4c, 4f and 7b) showed moderate activity (312.5, 312.5, 156.25 and, 156.25 μg/ml, respectively) and the others (3a, b and 4a, b) are inactive against two types of bacteria. On the other hand, Compounds 4c and 7b showed potent antifungal activity against yeast *Candida albicans* with MIC 78.12 (μg/ml). In addition, two compounds 4d and 4e revealed a moderate activity valued 156.25 and 156.25 [30] (μg/ml) with *Candida albicans*. In a comparison with the starting materials 1a, b, compound 4c is the most potent antibacterial pyrazolone derivative due to the presence of isopropyl-group which might be responsible for the activity [31]. On the other side, the most potent antifungal activity related to compounds 4c and 7b that contains two *N*-dimethyl groups which enhance the activity of antifungal property [32, 33]. So, the chain length of alkyl group

Egypt. J. Chem. 69, No. 2 (2026)

improves the antimicrobial activity. The potential activities of the new compounds can be controlled by the cell outer layers of these [34] two types of bacteria. Gram (+) bacteria has an inadequate and permeable peptidoglycan layer as their outer barrier. Therefore, drug components can pass through the Gram (+) bacteria's cell wall. However, the cell wall of Gram (-) bacteria are composed of a multilayered peptidoglycan and phospholipidic membrane that is impervious to drug components [35]. Nevertheless, compounds (4c, 4e, 4f and 7b) have a good activity against *E. coli* due to their potent structure that docked in the active site.

# 2.3. DFT study:

# **Optimized Geometry:**

The optimized geometry of novel synthesized structures from 1(a,b), 3 (a,b), 4 (a-f) and 7 (a,b)\_derivatives were studied in gas phase via B3LYP/ 6-311G (d,p) method. The optimized molecular structures of all compounds were presented in Figure 2.

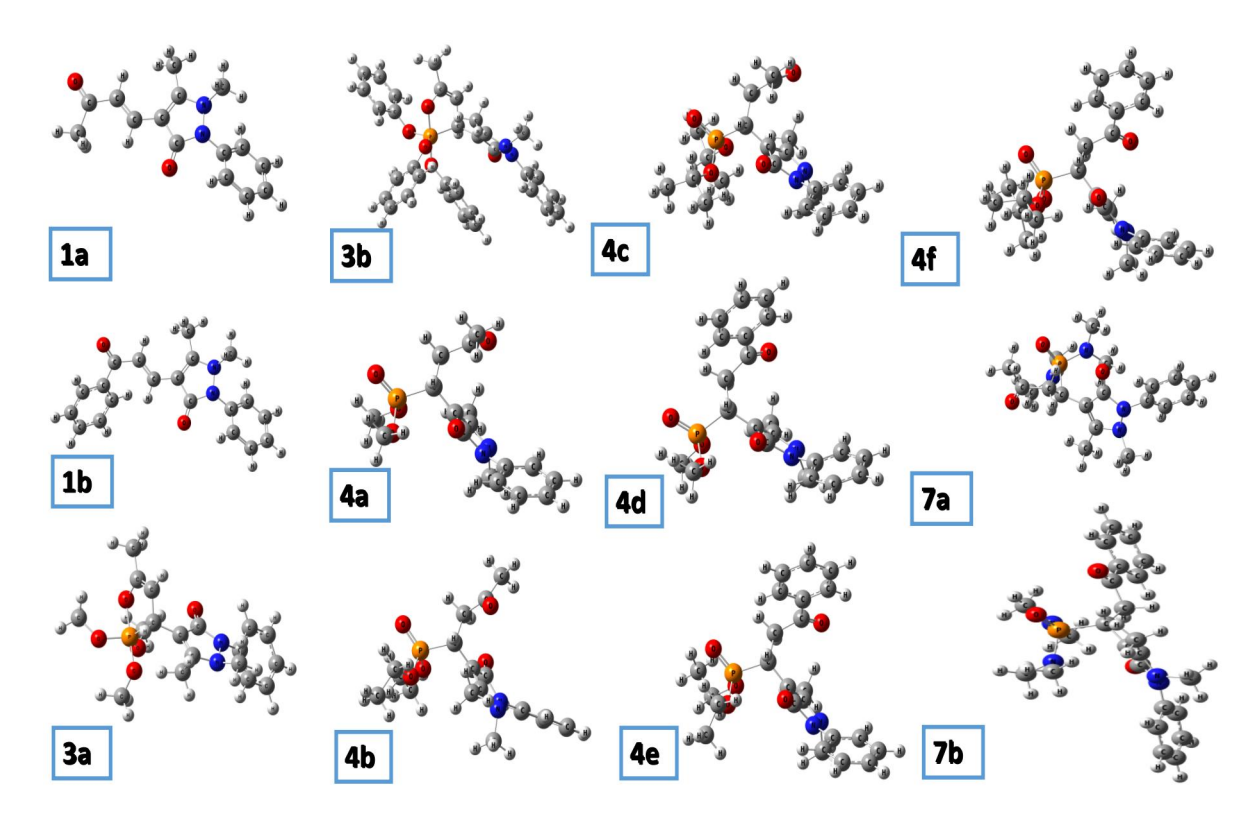


**Figure 2**. The optimized molecular structure of novel dimethyl-trimethoxy-oxaphosphol-pyrazol-3-one and dimethylpyrazoloxobutylphosphonate derivatives, as a ball-and-stick model colored by atom.

# Frontier molecular orbitals and global reactivity descriptors

The structures of all new synthesized compounds have been fully optimized via DFT/B3LYP/6–311G (d,p) level of theory in order to study the electronic behavior of the compounds and hence their chemical reactivity. The highest occupied molecular orbital (HOMO) and the Lowest unoccupied molecular orbital (LUMO) were studied to show the electronic effects properties based on DFT studied in order to evaluate the structural properties of the new compounds [36, 37]. The HOMO is related to the electrons in the outermost orbital and tends to donate electrons, meanwhile the LUMO is the orbital without outermost electrons and tends to gain electrons. The HOMO energy represents ionization energy and the LUMO represents electron activation energy. The energy different between the HOMO and LUMO energies is known as energy gap (ΔE) which represents the chemical reactivity and stability of the compounds. The smaller the band gap the more active will be the compounds. The HOMO and LUMO shapes illustrate the mode of interaction of the synthesized molecules based on electronic

interaction properties which illustrate the intramolecular charge transfer. In the present study the physical descriptors had been detected to illustrate the reactivity of the phosphorus compounds based on the energy of HOMO and LUMO orbitals as shown in figure 2 and their values were presented in table 3.

The HOMOs of starting prazolone (1a and 1b) are localized over the whole molecule, meanwhile the LUMO is located at pyrazone moiety. Compound 3a had the smallest band gap due to complete separation of HOMO and LUMO nodes. The HOMO of 3a is localized mainly on phosphonate part and the LUMO is over pyrazolone part with destabilization of LUMO and stabilization of HOMO compared with 1a and 1b. Although the phenyl group of 3b leads to stabilize the HOMO and destabilize the LUMO and increasing of the band gap and both HOMO and LUMO were located at pyazolone-phosphonate moieties. The new class of derivatives from (4a-4e), the HOMOs are delocalized over pyrazolone derivatives and the LUMOs were localized over pyrazolone moiety, except for phenyl-R' substituted compounds (4d-4f), the LUMOs were located over phenyl group. The band gaps showed values (from 4.11 eV to 5.08) in which HOMOs energies were destabilized and LUMOs energies were stabilized, especially with phenyl-R' substitutions. The phosphor-propanoyl (7a and 7b) derivatives were new classes of compounds that show HOMOs with different circulation figures as both have HOMOs over phosphonates and LUMOs over pyrazolone in case of 7a and phenyl in case of 7b. The band gap values are moderated compared to references (1a and 1b) and other phosphorus material (3a-4f).

**Table 3.** Theoretical Energy Calculations and Dipole Moment of the Studied Compounds

Table	3. Theoretical	Energy Cal	culations an	a Dipole I	vioment o	the Stud	ied Compo	unas.		
ID	E (aV)	energy (eV)								
ID	E <sub>total</sub> (eV)	Е номо	E <sub>LUMO</sub>	ΔE	I	A	η	S	μ	X
1a	-841.367	-6.216	-2.174	4.042	6.216	2.174	-2.021	-0.495	-1.587	4.195
1b	-1033.145	-6.206	-2.222	3.985	6.206	2.222	-1.992	-0.502	-1.611	4.214
3a	-4586.465	-5.517	-0.755	4.761	5.517	0.755	-2.381	-0.420	-0.878	3.136
<b>3</b> b	-5242.165	-5.731	-0.901	4.830	5.731	0.901	-2.415	-0.414	-0.950	3.316
4a	-1646.324	-6.074	-0.997	5.077	6.074	0.997	-2.538	-0.394	-0.999	3.536
4b	-1567.667	-5.289	-0.686	4.602	5.289	0.686	-2.301	-0.435	-0.843	2.987
4c	-1646.324	-6.042	-0.981	5.061	6.042	0.981	-2.530	-0.395	-0.990	3.511
4d	-1680.788	5.061	-1.798	4.150	-5.061	1.798	3.429	0.292	-1.399	-1.631
4e	-1759.448	-5.932	-1.790	4.142	5.932	1.790	-2.071	-0.483	-1.395	3.861
4f	-1838.106	-5.928	-1.816	4.112	5.928	1.816	-2.056	-0.486	-1.408	3.872
7a	-1527.871	-5.985	-1.056	4.929	5.985	1.056	-2.465	-0.406	-1.028	3.520
7b	-1719.642	-5.913	-1.634	4.279	5.913	1.634	-2.140	-0.467	-1.317	3.773

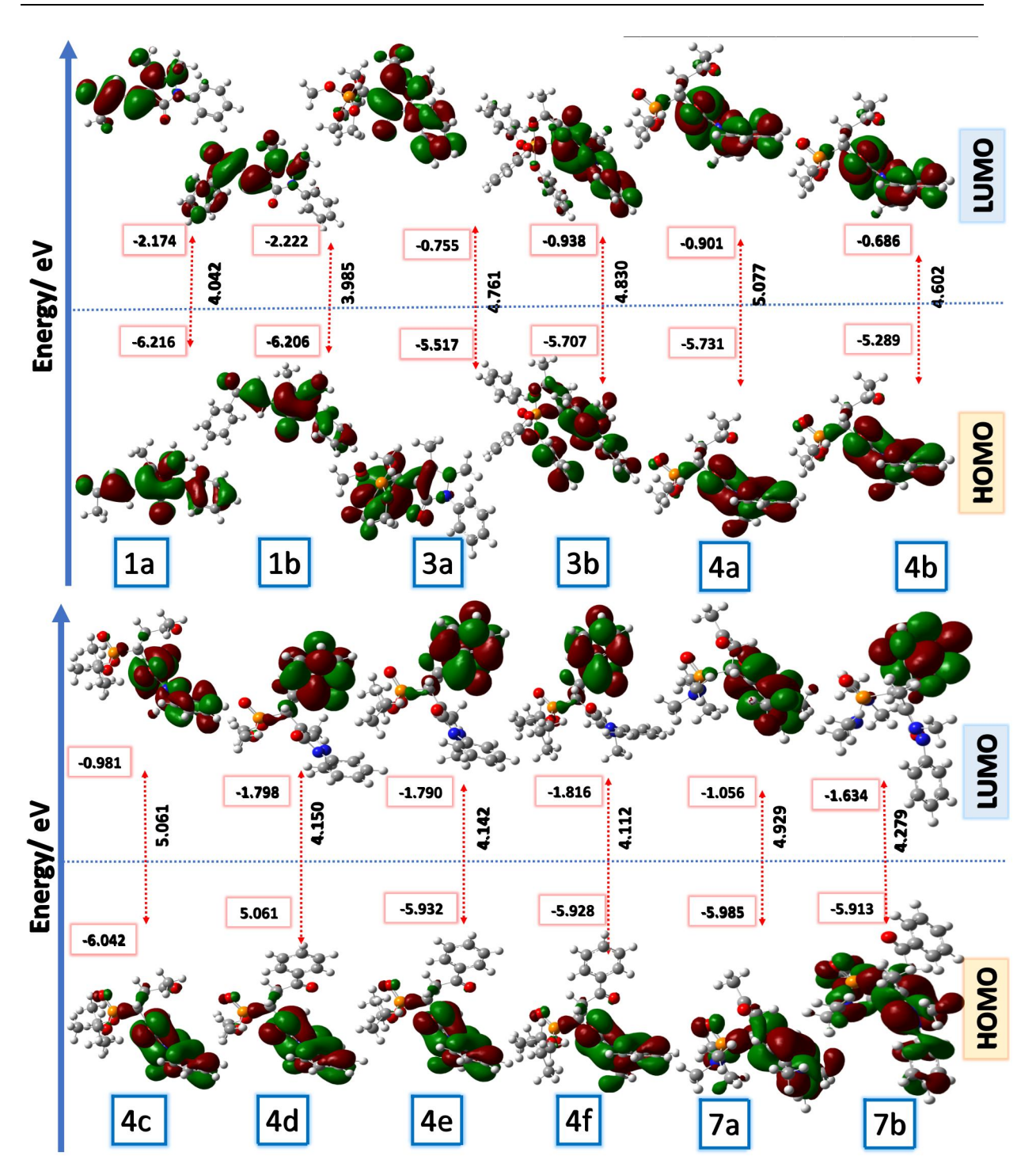


**Figure 3.** Frontier molecular orbitals for all novel dimethyl-trimethoxy-oxaphosphol-pyrazol-3-one and dimethylpyrazoloxobutylphosphonate derivatives calculated in gas phase at B3LYP/6-311G (d,p) method; Energy level of HOMOs and LUMOs and  $E_{gap}$  ( $\Delta E$ ).

# Molecular Electrostatic Potential (MEP) Maps

Molecular electrostatic potential (MEP) is a very powerful tool utilized to determine the reactive regions of nucleophilic and electrophilic attacks on a molecular system based on their charge distribution and polarization along with capability of Hydrogen-bond formation. It can be generated by mapping the electrostatic potential on to the isoelectron density surface of the molecule, which gives us the possibility to determine the distribution of the electronic charge over all the structure. Essentially, MEP mapping remains a useful way to give a clear imagination of the system and therefore its interaction with its environment as well as the biological recognition

processes.[38] In the present study, the MEP maps of all compounds show good nucleophilic behavior based on the color map presented in figure 3. The colors denote the reactivity of the region; blue is most positive electrostatic potential, red (represent electrophilic reactivity) > orange > yellow > green > blue (nucleophilic reactivity). From the MEP plots it was presumed that all phosphonate derivative parts showed high electropositive potential (red) and the *N-N* group of pyrazolone possessed slightly low electropositive region

reactivity). From the MEP plots it was presumed that all phosphonate derivative parts showed high electropositive potential (red) and the *N-N* group of pyrazolone possessed slightly low electropositive region (blue). Accordingly, the phosphonate group of all new synthesized compounds support electrophilicity pyrazolone moiety promotes nucleophilicity.

**1**a 1b 3a 3b 4a 4b **4c** 4d

Figure 4. Generated molecular electrostatic potential (MEP) maps of all studied compounds.

7a

# 2.4. Molecular docking study

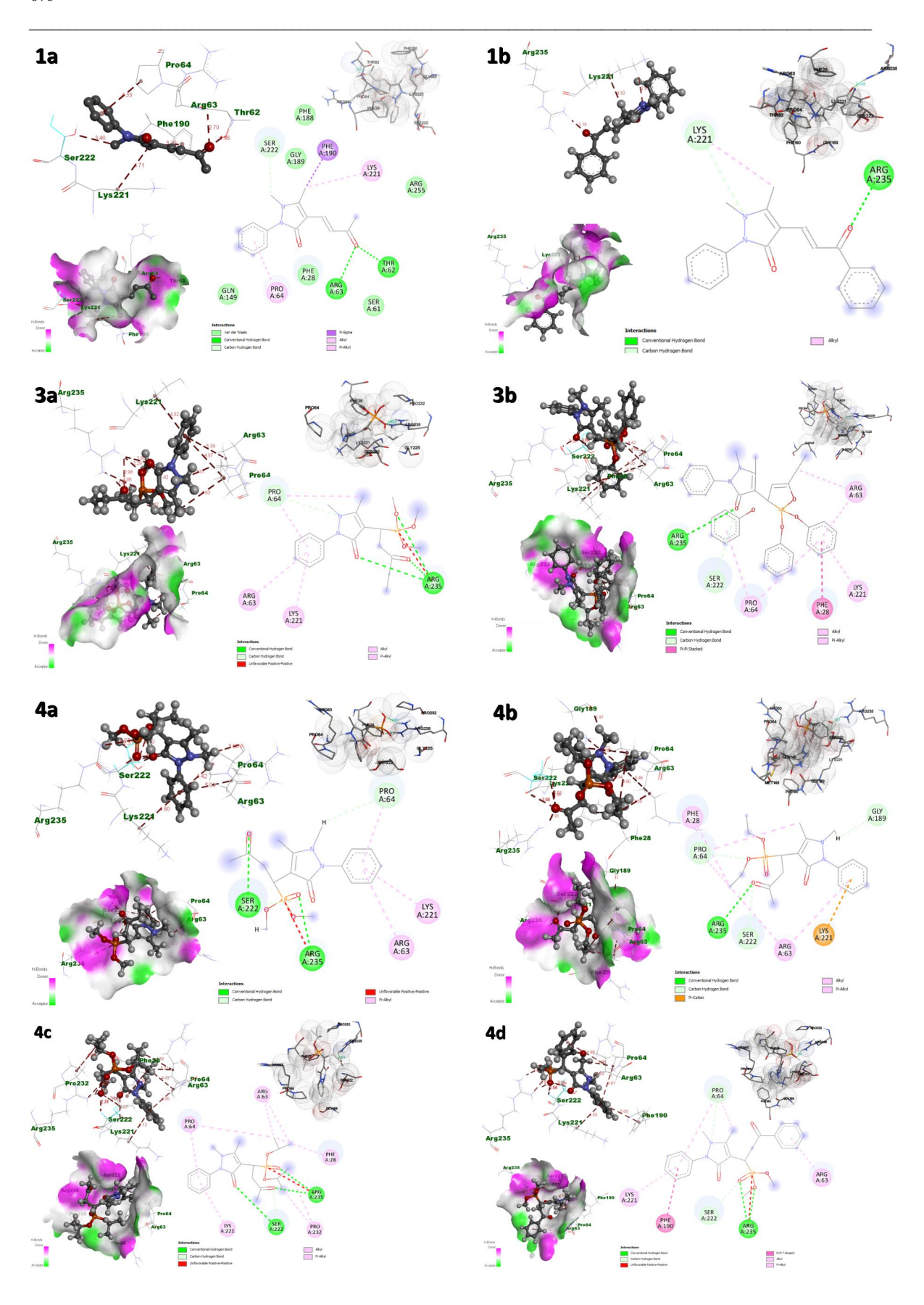
Molecular docking studies were carried out for all the synthesized compounds to evaluate the binding energies with dihydropteroate (DHPS). The dihydropteroate synthase is one of the enzymes involved in the bacterial folate synthesis pathway. The folate synthesis pathway is an essential pathway for synthesizing amino acids.[39, 40] The DHPS had two characteristic binding sites: the first one binds with dihydropterin pyrophosphate (DHPP) and the second one binds with p-amino benzoic acid (pABA).[41, 42] The most important amino acids residues for the first type which interact with protein moiety are (Asp96, Asn115, Asp185, Lys221 and Arg235). Meanwhile, the second serious of amino acids that interact with pABA moiety are (Phe190, Lys221 and Ser222).[43, 44] All the synthesized compounds were found to have strong interaction with the with hydropteroate (DHPS) with inhibition constant range from (4.19-560.27  $\mu$ M) as shown in table 4. All compounds show H-bond interaction with Arg235 and some Pi-Pi interaction with other amino acids. Except for the high potent compounds 4c, 4e, 4f and 7b, they have another strong H-bond interaction with Lys221 and more Pi-Pi interactions. This is the reason why their potency as antimicrobial agents were very high compared to other derivatives. The formed H-bonds visualized to oriente with the whole active site as depicted in figure 6.

Table 4. Docking score and binding energy (kcal/mol) of studied ligands with the referent ligand.

No.	Code number	Chemical structure	Binding Energy (µM)	Ki	RMSD
	1a	N. N O	-6.74	11.47	44.34
	1b	O N,NO	-7.34	4.19	43.10
	3a	P(OCH <sub>3</sub> ) <sub>3</sub>	-5.9	45.21	41.27

3b	P(OCH <sub>3</sub> ) <sub>3</sub>	-7.35	4.11	42.01
<b>4</b> a	P-OCH <sub>3</sub> OCH <sub>3</sub>	-6.37	21.43	41.80
4b	O P-OCH <sub>2</sub> CH <sub>3</sub> OCH <sub>2</sub> CH <sub>3</sub>	-7.16	5.61	43.36
<b>4c</b>	O P-OCH(CH <sub>3</sub> ) <sub>2</sub> OCH(CH <sub>3</sub> ) <sub>2</sub>	-6.10	33.78	42.77
4d	O P-OCH <sub>3</sub> OCH <sub>3</sub>	-7.33	4.25	42.70

<b>4</b> e	O P-OCH <sub>2</sub> CH <sub>3</sub> OCH <sub>2</sub> CH <sub>3</sub>	-5.41	107.52	45.89
4f	O P-OCH(CH <sub>3</sub> ) <sub>2</sub> OCH(CH <sub>3</sub> ) <sub>2</sub>	-4.44	560.27	45.10
7a	O O O O O O O O O O O O O O O O O O O	-5.98	41.03	42.99
7b	O N N N N N N N N N N N N N N N N N N N	-6.79	10.59	43.13



Egypt. J. Chem. 69, No. 2 (2026)

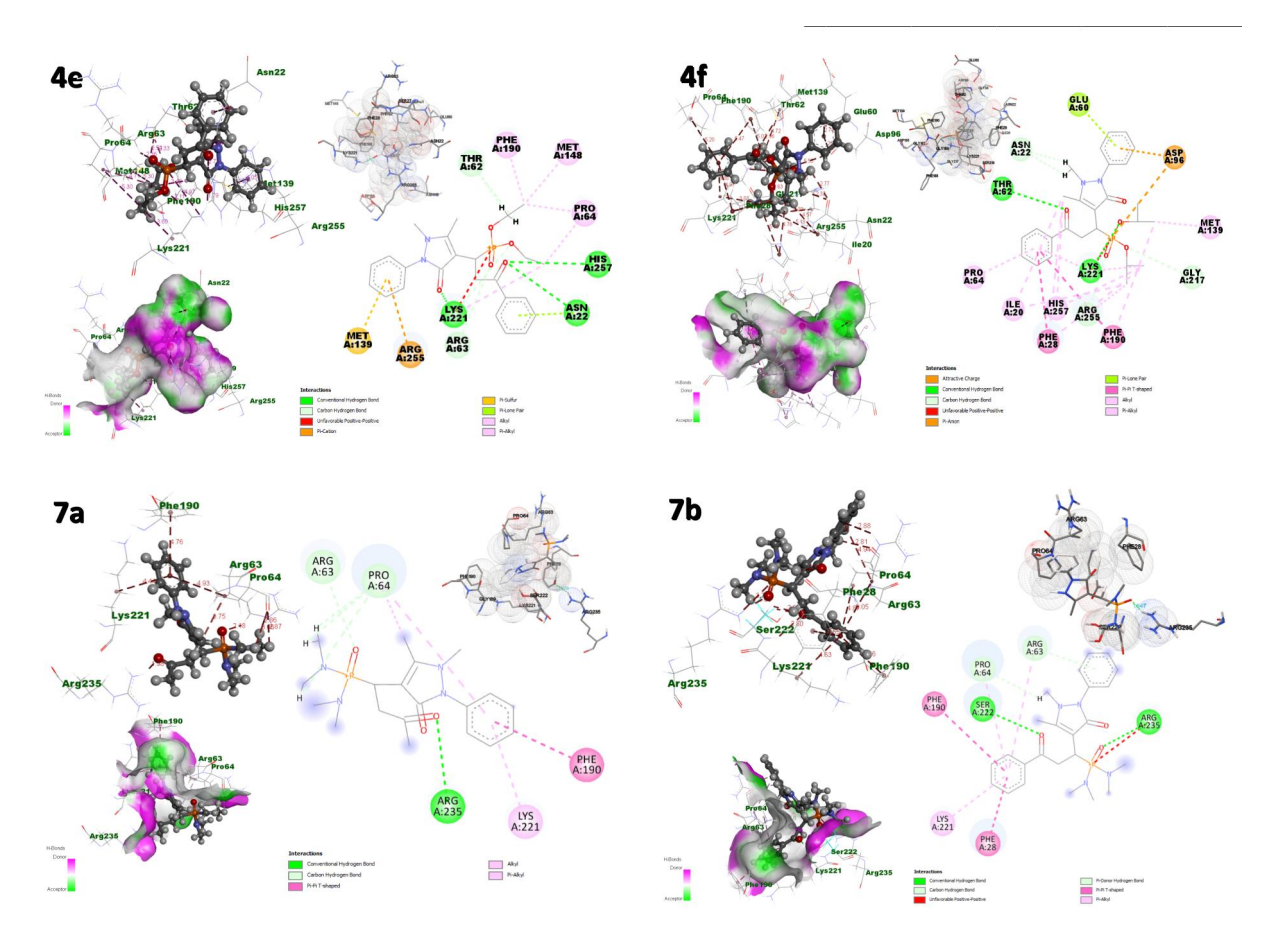


**Figure 5.** 3D and 2D Docking pose of docked derivatives into DHPS; A: compound 3a (purple), B: compound 3b (pink), C: compound 3c (green) and D: compound 3d (orange). H-Bond interactions shown in green line.

# 3. Experimental

# 3.1. Chemistry

Melting points were determined in open glass capillaries using an Electrothermal IA 9100 series digital melting point apparatus (Electrothermal, Essex, UK), and IR spectra were measured as KBr pellets with a PerkinElmer Infrared Spectrophotometer model 157. The <sup>1</sup>H, <sup>13</sup>C and <sup>31</sup>P NMR spectra were recorded in CDCl<sub>3</sub> or [d<sub>6</sub>] DMSO as solvents on a Jeol-500 spectrometer (<sup>1</sup>H: 500 MHz; <sup>13</sup>C: 125 MHz), and the chemical shifts are recorded in δ values relative to TMS as internal reference. The mass spectra were recorded at 70 eV with a Kratos MS equipment or a Varian MAT 311A spectrometer. Elemental analyses were performed using an Elementar Vario E1 instrument. The reported yields are of pure isolated materials obtained by column chromatography on silica gel 60 (Merck).

# General experimental

See supplementary file

Solvent-free synthesis of phosphonates

Compounds **1a**, **b** (1 mmol) and phosphorus compounds **2a**,**b**, **5a**-**c** and **6** (1.2 mmol) were added to Pd acetate (0.05 g) and the mixture was heated in an oil bath at 50°C. The progress of the reaction was monitored by *TLC*. After the reaction was complete, purification using column chromatography (ethyl acetate/n-hexane) to give **3a**,**b**, **4a**-**f** and **7a**,**b**.

1,5-Dimethyl-4-(2,2,2-trimethoxy-5-methyl-2,3-dihydro-1,2-oxaphosphol-3-yl)-2-phenyl-1,2-dihydro-3H-pyrazol-3-one (**3a**)

This product was isolated from column chromatography using petroleum ether 60-80 °C / ethyl acetate (70: 30 v/v) as an eluent, pale yellow crystals, yield 25%, m.p.: 141-143°C. IR (KBr, cm<sup>-1</sup>):.  $\tilde{V}$  =1681 (C=O, pyrazolone), 991 (P-OCH<sub>3</sub>). <sup>1</sup>H NMR (500 MHz,  $d_{6}$ - DMSO,  $\delta$ , ppm): 7.28- 7.48 (m, 5 H, H-arom.), 4.18 (d, 1H, CH), 3.66- 3.43 (m, 10 H, 3 OCH<sub>3</sub> + CH), 3.10 (s, 3 H, N-CH<sub>3</sub>), 2.14 (s, 3H, CH<sub>3</sub>), 1.18 (d, 3 H, O-C- CH<sub>3</sub>). <sup>13</sup>C NMR (125

MHz,  $d_{\sigma}$ -DMSO,  $\delta$ , ppm): 163.97 (C=O), 135.80-124.29 (arom. -C), 53.85 (OCH<sub>3</sub>), 36.12 (*N*-CH<sub>3</sub>), 14.84 (CH<sub>3</sub>), 11.98 (CH<sub>3</sub>). <sup>31</sup>P NMR (200 MHz,  $d_{\sigma}$ -DMSO,  $\delta$ , ppm): 33.27. MS (EI, 70 eV): m/z (%): 378 [M-2H]<sup>+</sup>, 3]. Anal. Calcd. for C<sub>18</sub>H<sub>25</sub>N<sub>2</sub>O<sub>5</sub>P (380.38). Calcd: C, 56.84; H, 6.62; N, 7.36; P, 8.14. Found: C, 56.77; H, 6.56; N, 7.31; P, 8.03.

1,5-Dimethyl-4-(2,2,2-trimethoxy-5-phenyl-2,3-dihydro-1,2-oxaphosphol-3-yl)-2-phenyl-1,2-dihydro-3H-pyrazol-3-one (3b)

This product was isolated from column chromatography using pet.ether 60-80/ ethyl acetate (70: 30 v/v) as an eluent, pale yellow crystals, yield 25%, m.p: 214-216 °C. IR (KBr, cm<sup>-1</sup>):  $\tilde{V} = 1619$  (C=O, pyrazolone), 1010 (P-OCH<sub>3</sub>). <sup>1</sup>H NMR (500 MHz,  $d_{\sigma}$  DMSO,  $\delta$ , ppm): 8.04 - 7.35 (m, 10 H, H-arom. ), 4.10 (d, 1H, CH), 3.21 (s, 10 H, 3 OCH<sub>3</sub> + CH), 3.21 (s, 3 H, *N*-CH<sub>3</sub>), 2.47 (s, 3H, CH<sub>3</sub>), 1.20 (s, 3 H,O-C-CH<sub>3</sub>). <sup>13</sup>C NMR (125 MHz,  $d_{\sigma}$ -DMSO,  $\delta$ , ppm): 167.74 (C=O), 132.25-128.39 (arom.-C), 65.54 (OCH<sub>3</sub>), 39.91 (*N*-CH<sub>3</sub>), 19.18 (CH<sub>3</sub>), 14.05 (CH<sub>3</sub>). MS (EI, 70 eV): m/z (%) 441 [M-H]<sup>+</sup>, 1]. Anal. Calcd. for C<sub>23</sub>H<sub>27</sub>N<sub>2</sub>O<sub>5</sub>P (442.44). Calcd: C, 62.44; H, 6.15; N, 6.33; P, 7.00. Found: C, 62.36; H, 6.10; N, 6.28; P, 6.92

Dimethyl(1-(1,5-dimethyl-3-oxo-2-phenyl-2,3-dihydro-1H-pyrazol-4-yl)-3-oxobutyl)phosphonate (4a)

This product was isolated from column chromatography using pet.ether 60-80/ ethyl acetate (70: 30 v/v) as an eluent, pale yellow crystals, yield 25%, m.p.: 156-158 °C. IR (KBr, cm<sup>-1</sup>):  $\widetilde{V}=1743$  (C=O, pyrazolone), 1589 (C=O, broad), 1238 (P=O), 1103 (P-OCH<sub>3</sub>). H NMR (500 MHz, DMSO- $d_6$ ,  $\delta$ , ppm): 7.45 - 7.25 (m, 5 H, H-arom. ), 3.70-3.35 (m, 8 H, 2 OCH<sub>3</sub>+CH<sub>2</sub>), 3.29 (m, 1H J<sub>HP</sub>= 10 Hz, CH-P), 2.99 (s, 3 H, N-CH<sub>3</sub>), 2.25 (s, 3H, CH<sub>3</sub>), 2.04 (s, 3 H,O-C-CH<sub>3</sub>). The NMR (125 MHz,  $d_6$ -DMSO,  $\delta$ , ppm): 205.38 (CH<sub>3</sub>-C=O), 164.51 (C=O), 129.17-123.65 (arom.-C), 53.06 (OCH<sub>3</sub>), 36.11 (N-CH<sub>3</sub>), 30.30 (CH<sub>3</sub>), 11.99 (CH<sub>3</sub>). The NMR (200 MHz,  $d_6$ -DMSO,  $\delta$ , ppm): 21.03. MS (EI, 70 eV): m/z (%) 365 [M-H]<sup>+</sup>, 2]. Anal. Calcd. for C<sub>17</sub>H<sub>23</sub>N<sub>2</sub>O<sub>5</sub>P (366.35). Calcd: C, 55.73; H, 6.33; N, 7.65; P, 8.45. Found: Calcd: C, 55.67; H, 6.28; N, 7.59; P, 8.38.

Diethyl(1-(1,5-dimethyl-3-oxo-2-phenyl-2,3-dihydro-1H-pyrazol-4-yl)-3-oxobutyl)phosphonate (4b)

This product was isolated from column chromatography using pet.ether 60-80/ ethyl acetate (50: 50 v/v) as an eluent, colorless crystals, yield 25%, m.p:120-122 °C. IR (KBr, cm<sup>-1</sup>):  $\tilde{V}$  =.1720 (C=O, pyrazolone), 1592 (C=O), 1181(P=O), 1118 (P-O-CH<sub>2</sub>). <sup>1</sup>H NMR (500 MHz,  $d_6$ - DMSO,  $\delta$ , ppm): 7.97 – 6.98 (m, 5 H, H-arom.), 3.96 (q, 4 H, CH<sub>3</sub>CH<sub>2</sub>-O-), 3.06-1.93 (m, 12 H, CH-P + CH<sub>2</sub>+ N-CH<sub>3+2</sub> CH<sub>3</sub>), 1.14 (t, 6H, CH<sub>3</sub>CH<sub>2</sub>-O-). <sup>13</sup>C NMR (125 MHz,  $d_6$ -DMSO,  $\delta$ , ppm): 195.42 (CH<sub>3</sub>-C=O), 149.87 (C=O), 133.42-127.71 (arom.-C), 64.01 (CH<sub>3</sub>CH<sub>2</sub>-O-), 42.8 (N-CH<sub>3</sub>), 39.5 (O=C-CH<sub>3</sub>), 25.30 (CH<sub>3</sub>), 10.58 (CH<sub>3</sub>CH<sub>2</sub>-O-). MS (EI, 70 eV): m/z (%) 395 [M+H]<sup>+</sup>, 21]. Anal. Calcd. for C<sub>19</sub>H<sub>27</sub>N<sub>2</sub>O<sub>5</sub>P (394.40). Calcd: C, 57.86; H, 6.90; N, 7.10; P, 7.85. Found: C, 57.75; H, 6.85; N, 6.95; P, 7.72.

Diisopropyl(1-(1,5-dimethyl-3-oxo-2-phenyl-2,3-dihydro-1H-pyrazol-4-yl)-3-oxobutyl) phosphonate (4c) This product was isolated from column chromatography using pet.ether 60-80/ ethyl acetate (85: 15 v/v) as an eluent, pale yellow crystals, yield 25%, m.p. 236-238 °C. IR (KBr, cm<sup>-1</sup>):  $\tilde{V}$  =1635 (C=O, pyrazolone), 1592 (C=O, broad), 1222 (P=O), 1022 (P-O-CH). <sup>1</sup>H NMR (300 MHz,  $d_6$ -DMSO,  $\delta$ , ppm): 7.40 - 7.22 (m, 5 H, Harom.), 4.51-4.53 (m, 2 H, 2 CH, isopropyl), 3.31-2.90 (m, 6 H, N-CH<sub>3</sub>+ CH-P + CH<sub>2</sub>), 2.36 (s, 3H, CH<sub>3</sub>), 2.21 (s, 3 H,O-C-CH<sub>3</sub>), 1.22-1.18 (m, 12 H, 4 CH<sub>3</sub>, isopropyl). <sup>13</sup>C NMR (125 MHz, d<sub>6</sub>-DMSO, δ, ppm): 183.85 (CH<sub>3</sub>-C=O), 161.51 (C=O), 134.05-120.36 (arom.-C), 70.22 (-CH(CH<sub>3</sub>)<sub>2</sub>), 60.32 (CH<sub>2</sub>), 33.19 (N-CH<sub>3</sub>), 28.06 (O=C-CH<sub>3</sub>), 23.84 (4 CH<sub>3</sub>, isopropyl), 10.34 (CH<sub>3</sub>). MS (EI, 70 eV): m/z (%) 422 [M]<sup>+</sup>, 8]. Anal. Calcd. for C<sub>22</sub>H<sub>31</sub>N<sub>2</sub>O<sub>5</sub>P (422.46). Calcd: C, 59.70; H, 7.40; N, 6.63; P, 7.33. Found: C, 59.64; H, 7.37; N, 6.55; P, 7.27. Dimethyl(1-(1,5-dimethyl-3-oxo-2-phenyl-2,3-dihydro-1H-pyrazol-4-yl)-3-oxo-3-phenylpropyl)phosphonate (4d) This product was isolated from column chromatography using pet.ether 60-80/ ethyl acetate (85: 15 v/v) as an eluent, pale yellow crystals, yield 25%, m.p.: 145-147 °C. IR (KBr, cm<sup>-1</sup>):  $\tilde{V}$  = 1639 (C=O, pyrazolone), 1592 (C=O), 1006 (P-OCH<sub>3</sub>), 1295 (P=O). <sup>1</sup>H NMR (500 MHz,  $d_{6}$ - DMSO,  $\delta$ , ppm): 7.88 - 7.25 (m, 10 H, H-arom.), 4.22-4.17 (m, 1 H, CH), 3.52 (d, 8 H, (P-O-CH<sub>3</sub>)<sub>2</sub>),  $J_{CP} = 15$  Hz + CH<sub>2</sub>), 3.03 (s, 3H, N-CH<sub>3</sub>), 2.47 (s, 3 H, CH<sub>3</sub>). <sup>13</sup>C NMR (125 MHz, d6-DMSO,  $\delta$ , ppm): 184.24 (Ph-C=O), 161.09 (C=O), 136.09-127.44 (arom.-C), 67.26 (P(OCH<sub>3</sub>)<sub>2</sub>), 33.10 (N-CH<sub>3</sub>), 25.3 (CH<sub>3</sub>). MS (EI, 70 eV): m/z (%) 396 [M-CH<sub>3</sub>OH]<sup>+</sup>, 23]. Anal. Calcd. for C<sub>22</sub>H<sub>25</sub>N<sub>2</sub>O<sub>5</sub>P (428.42). Calcd: C, 61.68; H, 5.88; N, 6.54; P, 7.23. Found: C, 61.55; H, 5.81; N, 6.49; P, 7.12. Diethyl(1-(1,5-dimethyl-3-oxo-2-phenyl-2,3-dihydro-1H-pyrazol-4-yl)-3-oxo-3-phenylpropyl)phosphonate (4e) This product was isolated from column chromatography using pet ether 60-80/ ethyl acetate (50: 50 v/v) as an eluent, colorless crystals, yield 25%, m.p.: 106-108 °C. IR (KBr, cm<sup>-1</sup>):  $\tilde{V}$  = 1639 (C=O, pyrazolone), 1589 (C=O), 1261 (P=O), 1110 (P-OCH<sub>2</sub>). <sup>1</sup>H NMR (300 MHz,  $d_{\theta}$ - CDCL<sub>3</sub>,  $\delta$ , ppm): 7.71 – 6.98 (m, 10 H, H-arom.), 4.24-2.35 (m, 10 H, 2 CH<sub>3</sub>CH<sub>2</sub>-O-+ CH<sub>2</sub>+CH-+*N*-CH<sub>3</sub>), 1.20 (t, 6 H, 2 CH<sub>3</sub>CH<sub>2</sub>-O-). <sup>13</sup>C NMR (125 MHz,  $d_6$ -DMSO, δ, ppm): 213.48 (Ph-C=O), 167.45 (C=O), 132.84-127.89 (arom.-C), 67.68, 38.30 (3 CH<sub>2</sub>), 35.53 (N-C)

CH<sub>3</sub>), 22.43 (CH<sub>3</sub>) 11.27, 14.40 (2 O-CH<sub>2</sub>-<u>CH<sub>3</sub></u>) MS (EI, 70 eV): m/z (%):456 [M]<sup>+</sup>, 52]. Anal. Calcd. for  $C_{24}H_{29}N_2O_5P$  (456.47). Calcd: C, 63.15; H, 6.40; N, 6.14; P, 6.79. Found: C, C, 63.06; H, 6.32; N, 6.09; P, 6.68 Diisopropyl(1-(1,5-dimethyl-3-oxo-2-phenyl-2,3-dihydro-1H-pyrazol-4-yl)-3-oxo-3-phenylpropyl) phosphonate (4f)

This product was isolated from column chromatography using pet.ether 60-80/ ethyl acetate (85: 15 v/v) as an eluent, pale yellow crystals, yield 25%, m.p. 280-282°C. IR (KBr, cm<sup>-1</sup>):  $\tilde{V} = 1681$ (C=O, pyrazolone), 1619 (C=O), 1207 (P=O), 1099 (P-O-CH). <sup>1</sup>H NMR (500 MHz,  $d_6$ - DMSO,  $\delta$ , ppm): 7.40 - 7.22 (m, 10H, H-arom.), 4.51-4.53 (m, 2 H, 2 CH, isopropyl), 3.31-2.90 (m, 6 H, N-CH<sub>3</sub> + CH-P + CH<sub>2</sub>), 2.36 (s, 3H, CH<sub>3</sub>), 1.22-1.18 (m, 12 H, 4 CH<sub>3</sub>, isopropyl). <sup>13</sup>C NMR (125 MHz,  $d_6$ -DMSO,  $\delta$ , ppm): 198.16 (Ph-C=O), 163.97 (C=O), 136.79-123.94 (arom.-C), 76.95 (-CH(CH<sub>3</sub>)<sub>2</sub>), 71.19 (CH<sub>2</sub>), 35.53 (N-CH<sub>3</sub>), 23.81 (4 CH<sub>3</sub>, isopropyl), 11.50 (CH<sub>3</sub>). MS (EI, 70 eV): m/z (%): 483 [M-H]<sup>+</sup>, 100] Anal. Calcd. for C<sub>26</sub>H<sub>33</sub>N<sub>2</sub>O<sub>5</sub>P (484.52). Calcd: C, 64.45; H, 6.86; N, 5.78; P, 6.39. Found: C, 64.28; H, 6.77; N, 5.66; P, 6.29.

3-[Bis(dimethylamino)phosphoryl]-3-(2-phenyl-1,5-dimethyl-3-oxo-2,3-dihydro-1H-pyrazol-4-yl)propanoyl methane (7a)

This product was isolated from column chromatography using pet.ether 60-80/ ethyl acetate (85: 15 v/v) as an eluent, pale yellow crystals, yield 25%, m.p.: 128-130 °C. IR (KBr, cm<sup>-1</sup>):  $\tilde{V} = 1720$ .(C=O, pyrazolone), 1592 (C=O), 1311, 755 (P-N(CH<sub>3</sub>)<sub>2</sub>), 1184 (P=O). H NMR (500 MHz,  $d_{\sigma}$  DMSO,  $\delta$ , ppm): 7.39 - 7.20 (m, 5 H, H-arom.), 2.48-2.24 (m, 23 H, 5 N-CH<sub>3</sub>+ CO-CH<sub>3</sub> + CH<sub>2</sub>+-C-CH<sub>3</sub>), 3.25 (d, 1 H, CH). MS (EI, 70 eV): m/z (%) 392 [M]<sup>+</sup>, 1]. Anal. Calcd. for C<sub>19</sub>H<sub>29</sub>N<sub>4</sub>O<sub>3</sub>P (392.43). Calcd: C, 58.15; H, 7.45; N, 14.28; P, 7.89. Found: C, 57.99; H, 7.38; N, 14.18; P, 7.78.

3-[Bis(dimethylamino)phosphoryl]-3-(2-phenyl-1,5-dimethyl-3-oxo-2,3-dihydro-1H-pyrazol-4-yl)propanoyl benzene (7b).

This product was isolated from column chromatography using pet.ether 60-80/ ethyl acetate (85: 15 v/v) as an eluent, pale yellow crystals, yield 25%, m.p.: 151-153 °C. IR (KBr, cm<sup>-1</sup>):  $\widetilde{V}=1781$  (C=O, pyrazolone), 1673 (C=O), 1353, 744 (P-N(CH<sub>3</sub>)<sub>2</sub>), 1245 (P=O). H NMR (500 MHz,  $d_{\sigma}$ - DMSO,  $\delta$ , ppm): 7.65-7.22 (m, 10 H, H-arom.), 2.92-2.10 (m, 21 H, 5 N-CH<sub>3</sub>+ CH<sub>3</sub>+ CH<sub>2</sub> + CH). The CH<sub>3</sub> C NMR (125 MHz,  $d_{\sigma}$ -DMSO,  $\delta$ , ppm): 203.88 (Ph-C=O), 164.08 (C=O), 134.71-125.90 (arom.-C), 35.16-25.36 (P(N-CH<sub>3</sub>)<sub>3</sub>+ CH<sub>2</sub>), 12.06 (CH<sub>3</sub>). MS (EI, 70 eV): m/z (%) 423 [M-CH<sub>3</sub>NH<sub>2</sub>]<sup>+</sup>, 3]. Anal. Calcd. for C<sub>24</sub>H<sub>31</sub>N<sub>4</sub>O<sub>3</sub>P (454.50). Calcd: C, 63.42; H, 6.87; N, 12.33; P, 6.81. Found C, 63.33; H, 6.81; N, 12.27; P, 6.75.

# 3.2. Methodology antimicrobial

The antimicrobial activity of the synthesized compounds was assessed against *Staphylococcus aureus* ATCC 6538-P as G+ve bacteria, *Escherichia coli* ATCC 25933 as G-ve bacteria, *Candida albicans* ATCC 10231 as yeast and *Aspergillus niger* NRRL as filamentous fungi test microbe using cup agar diffusion method. Samples were prepared by dissolving 5mg in 2ml of DMSO. Nutrient agar plates were used in case of bacterial and yeast test microbes whereas potato dextrose plates were used in case of fungal test microbe. Each plate was inoculated with 0.1ml of 10<sup>5</sup>cells/ml from each microbial stock. Then plates were kept at low temperature (4°C) for 2-4 hours to allow maximum diffusion. The plates were incubated at 37°C for 24 hours for bacteria and at 30°C for 48 hours for the fungus in upright position to allow maximum growth of the organisms. The antimicrobial activity of the test agent was measured by detecting the diameter of zone of inhibition expressed in millimeter (mm). The experiment was carried out more than once and the reported mean was recorded.

# Determination of minimum inhibitory concentration (MIC) of tested compounds

Staphylococcus aureus ATCC 6538 (G+ve bacteria), Escherichia coli ATCC 25933 (G-ve bacteria) and Candida albicans ATCC 10231 were cultivated on nutrient broth medium. Cell pellets were collected by centrifugation under sterile condition after cultivating the test microbes for 24h. Cells were resuspended in sterile normal saline with optical density of 0.5 to 1.0 giving actual CFU number of about 106 cell/ml. Resazurin solution was prepared (675 mg in 40 mL of sterile distilled water) and sterilized by filtration through membrane filter (pore size  $0.22\mu m$ ).  $100~\mu L$  of the broth culture was distributed in all wells of the plate then  $100~\mu L$  stock concentration of 2.5mg/mL form each purified compound was pipetted into the first row of the plate and then two fold dilution has been done up to tenth dilution.  $10\mu L$  of resazurin indicator solution was added to each well and  $10\mu L$  of bacterial suspension (106cfu/mL) was added to each well. The plates were incubated at  $37^{\circ}C$  for 24 h. The colour change was then assessed visually. Any colour changes from purple to pink or colourless were recorded as positive. The lowest concentration at which colour change occurred was taken as the MIC value.

# 3.3. Computational Procedure:

#### **DFT** calculations

The current investigation discussed the optimization of novel dimethyl-trimethoxy-oxaphosphol-pyrazol-3-one and dimethylpyrazoloxobutylphosphonate derivatives using gaussian 16 program [45] for all computations. All the chemical structures from 1(a,b), 3 (a,b), 4 (a-f) and 7 (a,b) have been optimized using the B3LYP/6-311G(d,p) functional.[46-48] All compounds were in their minima with absence of imaginary frequency. Frontier molecular orbitals had been studied in the ground state to describe the electronic structural behavior of the synthesized compounds. Electrostatic potential maps[49] were analyzed to identify the interaction points of the compounds.

DFT based parameters such as, energy of HOMO ( $E_H$ ), energy of LUMO ( $E_L$ ), band gab ( $\Delta E$ ), absolute softness (S)[50]; which indicate the capability of the composite to form a covalent bonds, global hardness ( $\eta$ ); that related to the struggle of the system to exchange electronic charge with the environment, electrophilicity index ( $\omega$ ); which describes how does the stabilization energy of a given system affected via gains an additional electronic charge from the surrounding, nucleophilicity index (N); that is the inverse of the electrophilicity, ( $1/\omega$ ), chemical potential ( $\mu$ ); that regulates the tendency of the electrophile to accept more electronic charge, and are all calculated via DFT calculations.[51-53]

$\Delta E = E_{LUMO} - E_{HOMO}$	(1)
I=-E <sub>HOMO</sub>	(2)
A=-E <sub>LUMO</sub>	(3)
$\eta = \frac{(E_{HOMO} - E_{LUMO})}{2}$	(4)
$\sigma = 1/\eta$	(5)
$\sigma = \frac{1}{\eta}$ $\mu = \frac{-(1+A)}{2}$	(6)
$X=\frac{(I+A)}{2}$	(7)

Where,  $E_{HOMO}$  and  $E_{LUMO}$  represent the energies of HOMO and LUMO, respectively and  $\Delta E$ , is the band gab.

# Molecular docking study

The starting protein geometry of DHPS (Dihydroptorate Synthase of Versinia pestis, PDB ID 3TZF) was retrieved from the RCSB protein data bank (http://www.pdb.org) and following the next step to dock all the target geometry.

# Ligand preparation

☐ The optimized geometry obtained from gaussian was prepared using discovery studio along with the protein structure downloaded from protein data bank. Hydrogen and Gastegier charges were added for the ligand.

# Protein preparation

The structure of Dihydroptorate (PDB ID: 3TZF) was obtained from the RCSB protein Data Bank (<a href="https://www.rcsb.org/">https://www.rcsb.org/</a>). Discovery studio was used to identify and visualize the active compounds with protein. All the heteroatoms were removed and isolated from the 3TZF.pdb, to ensure that the receptor is free from any ligands before docking and hydrogen atoms were added to the typical geometry before docking. The solvent molecules in the protein were removed, hydrogen atoms, and Kollmann charges were added automatically via AutoDock software.

# Receptorgrid generation:

□A grid was generated using the Auto Dock 4.0 by selecting the active site residues in the protein (PDB ID: 3TZF).

# Docking using AutoDock

□The interaction mode of all new synthesized compounds and were predicted in the active site of 3TZF through rigid docking using AutoDock v 4.0. The compounds were docked to the receptor using the default settings of the Lamarckian genetic algorithm. After docking, the individual binding conformations of each ligand were observed, and the interactions with the protein were studied. The best and the most energetically favorable conformation of each compound were selected based on the fitness function that was optimized by the genetic algorithm. The results of the docking studies were quantified in terms of the binding energy (kcal/mol). The predicted binding free energy was used as criteria for ranking the compounds.

Egypt. J. Chem. 69, No. 2 (2026)

#### 4- Conclusion

The present study is considered an interesting approach to the synthesis of organophosphonate derivatives through the reaction of α, β-unsaturated compounds 1a,b with alkyl phosphites (2a,b and 5a-c) and phosphorus triamide 6. When substrates 1a,b reacted with trimethyl phosphite 2a gave two products 3a,b and 4a,b. But in case of the reaction of 2b and dialkyl phosphites 5a-c, gave the corresponding organophosphonate derivatives 4c-f. Moreover, tris(dimethylamino)-phosphorylpropanoylmethane and bis(dimethylamino)phosphoryl propanoylbenzene 7a,b respectively. Furthermore, the newly synthesized compounds 4c, 4e, 4f and 7d are screened as antibacterial, antifungal and they showed a good activity. Using DFT protocol study, HOMO-LUMO gaps and various chemical reactivity descriptors have been studied and explain the reactivity of the compounds. The results showed that compounds 4e and 4f have a good chemical reactivity. The electrostatic potential mapped was discussed to show the predicted site for both electrophilic and nucleophilic attack which influence antimicrobial activity. Moreover, the docking studies had been done to support the experimental hypothesis for all target compounds which agreed with their detected antimicrobial and antifungal by means of good binding energy and inhibition constant. High docking score and more interaction was observed for 4e, 4f and 7b indicated the high potency compared with the reference compound.

# **Declaration of Interest**

No known competing of interests (financially and non-financially) or personal relationships influencing the reported work were declared by the authors in this paper.

# **Consent to participate**

Not applicable

# **Consent for publication**

Not applicable

# **Data Availability**

Data is provided within the supplementary information files

# **Competing interests**

No known competing interests (financially and non-financially) or personal relationships influencing the reported work were declared by the authors in this paper.

# Funding

Not applicable

# **Authors' contributions**

Mansoura A. Abd-El-Maksoud, contributed to the preparation of newly designed organic compounds, writing the manuscript, and communicating with journals for publishing the manuscript. Basma Ghazal, Docking and DFT study, writing the manuscript. Mohamed S. Abdel-Aziz, contributed in antimicrobial activity for the newly prepared compounds and writing the manuscript. Marwa El-Hussieny, contributed the preparation of new designed organic compounds, writing the manuscript and communicates with journals for publishing the manuscript

# Acknowledgement

The authors would like to thank the National Research Centre for providing the equipment and facilities to carry out this practical work.

# 5- References

- [1] J.S. Ramos-Figueroa, N.D. Vetter, D.R. Palmer, Phosphonate and  $\alpha$ -fluorophosphonate analogs of d-glucose 6-phosphate as active-site probes of 11-myo-inositol 1-phosphate synthase, Methods in Enzymology, Elsevier2023, pp. 57-93.
- [2] M. Moullamri, K. Rharrabe, H. Annaz, A. Laglaoui, F. Alibrando, F. Cacciola, L. Mondello, N. Bouayad, S. Zantar, M.J.J.o.E.O.B.P. Bakkali, Salvia officinalis, Lavandula angustifolia, and Mentha pulegium essential oils: insecticidal activities and feeding deterrence against Plodia interpunctella (Lepidoptera: Pyralidae), 27 (2024) 16-33.
- [3] A.F.F. Gomes, Genomics of insecticide-metabolizing bacteria associated with Spodoptera frugiperda (Lepidoptera: Noctuidae) and their potential role in host detoxification, Universidade de São Paulo, 2024.
- [4] V.P. Kukhar, H.R. Hudson, Aminophosphonic and aminophosphinic acids: Chemistry and biological activity, John Wiley & Sons2000.
- [5] R.L.J. Hilderbrand, The role of phosphonates in living systems, DOI (1983).
- [6] D. Koszelewski, P. Kowalczyk, P. Śmigielski, J. Samsonowicz-Górski, K. Kramkowski, A. Wypych, M. Szymczak, R.J.M. Ostaszewski, Relationship between Structure and Antibacterial Activity of α-Aminophosphonate Derivatives Obtained via Lipase-Catalyzed Kabachnik– Fields Reaction, 15 (2022) 3846.

- [7] M. Voráčová, M. Zore, J. Yli-Kauhaluoma, P.J.B. Kiuru, M. Chemistry, Harvesting phosphorus-containing moieties for their antibacterial effects, 96 (2023) 117512.
- [8] N. K Sahu, S. S Balbhadra, J. Choudhary, D.J.C.m.c. v Kohli, Exploring pharmacological significance of chalcone scaffold: a review, 19 (2012) 209-225.
- [9] B. Salehi, C. Quispe, I. Chamkhi, N. El Omari, A. Balahbib, J. Sharifi-Rad, A. Bouyahya, M. Akram, M. Iqbal, A.O.J.F.i.P. Docea, Pharmacological properties of chalcones: A review of preclinical including molecular mechanisms and clinical evidence, 11 (2021) 592654.
- [10] S.S. Mukhtar, N.M. Morsy, A.S. Hassan, T.S. Hafez, H.M. Hassaneen, F.M.J.E.J.o.C. Saleh, A review of chalcones: synthesis, reactions, and biological importance, 65 (2022) 379-395.
- [11] R. Al-Saheb, S. Makharza, F. Al-Battah, R. Abu-El-Halawa, T. Kaimari, O.S.J.B.r. Abu Abed, Synthesis of new pyrazolone and pyrazole-based adamantyl chalcones and antimicrobial activity, 40 (2020) BSR20201950.
- [12] S. Farooq, Z.J.C.O.C. Ngaini, Chalcone derived pyrazole synthesis via one-pot and two-pot strategies, 24 (2020) 1491-1506.
- [13] H.A. Hofny, M.F. Mohamed, H.A. Hassan, E.S.M. Abdelhafez, G.E.D.A.J.A.d.P. Abuo-Rahma, A review of recent advances in anticancer activity and SAR of pyrazole derivatives, 358 (2025) e2400470.
- [14] I. Ameziane El Hassani, K. Rouzi, H. Assila, K. Karrouchi, M.h.J.R. Ansar, Recent advances in the synthesis of pyrazole derivatives: a review, 4 (2023) 478-504.
- [15] N.A. Elkanzi, H. Hrichi, R.A. Alolayan, W. Derafa, F.M. Zahou, R.B.J.A.o. Bakr, Synthesis of chalcones derivatives and their biological activities: a review, 7 (2022) 27769-27786.
- [16] M.A. Shalaby, S.A. Rizk, A.M.J.O. Fahim, B. Chemistry, Synthesis, reactions and application of chalcones: a systematic review, 21 (2023) 5317-5346.
- [17] F. Rahman, R. Ali, S. Tabrez, A. Mobeen, S.K. Akand, M. Arish, A.F. AlAsmari, N. Ali, A.J.C.B. Rub, D. Design, Exploration of potential inhibitors for autophagy-related protein 8 as antileishmanial agents, 99 (2022) 816-827.
- [18] M. Abd-El-Maksoud, M. El-Hussieny, H. Awad, A.-T.H. Mossa, F. Soliman, Chemistry of phosphorus ylides. Part 47. Synthesis of organophosphorus and selenium pyrazolone derivatives, their antioxidant activity, and cytotoxicity against MCF7 and HepG2, Russian Journal of General Chemistry, 90 (2020) 2356-2364.
- [19] M. Ali, M. El-Gendy, Synthesis of New Organophosphorus Pyrazole Derivatives as Human Myeloblastic Leukemia HL60 Cytotoxic Agents, Egyptian Journal of Chemistry, 65 (2022) 27-37.
- [20] M. El-Hussieny, M.A. Abd-El-Maksoud, F.M. Soliman, M.A. Fouad, M.K. El-Ashrey, Dual-target ligand discovery for Alzheimer's disease: triphenylphosphoranylidene derivatives as inhibitors of acetylcholinesterase and β-amyloid aggregation, Journal of Enzyme Inhibition and Medicinal Chemistry, 38 (2023) 2166040.
- [21] M. Abd-El-Maksoud, S. Maigali, H. Awad, M. El-Hussieny, Synthesis, Characterization, and Anticancer Evaluation of Some Heterocycles Bearing Chloroquinoline Moiety, Russian Journal of General Chemistry, 92 (2022) 2740-2754.
- [22] M. El-Hussieny, S.T. Mansour, A.I. Hashem, M.A. Fouad, M.A. Abd-El-Maksoud, Design, synthesis, and biological evaluation of new heterocycles bearing both silicon and phosphorus as potent MMP-2 inhibitors, Journal of the Chinese Chemical Society, 69 (2022) 1908-1923.
- [23] S.T. Mansour, M.A. Abd-El-Maksoud, M. El-Hussieny, H.M. Awad, A.I. Hashem, Efficient Synthesis and Antiproliferative Evaluation of New Bioactive N-, P-, and S-Heterocycles, Russian Journal of General Chemistry, 92 (2022) 1761-1774.
- [24] M.A. Abd-El-Maksoud, T.K. Khatab, S.S. Maigali, F.M. Soliman, A.A. Hamed, Chemistry of phosphorus ylides: Part 46—Efficient synthesis and biological evaluation of new phosphorus, sulfur, and selenium pyrazole derivatives, Journal of Heterocyclic Chemistry, 55 (2018) 2883-2892.
- [25] S.T. Mansour, A.I. Hashem, M.A. Abd-El-Maksoud, M. El-Hussieny, A.I. El-Makawy, S.H. Abdel-Aziem, F.M. Soliman, The synthesis and antineoplastic activities of thiaziridine, sulfidometylphosphonium, and dithiaphosphitane-sulfide against the Ehrlich ascites carcinoma, Fundamental & Clinical Pharmacology, 36 (2022) 536-552.
- [26] B. Arbuzov, A. Fuzhenkova, G. Tudrii, Reaction of trimethyl phosphite with benzalacetophenone and benzal-α-tetralone, Bulletin of the Academy of Sciences of the USSR, Division of chemical science, 25 (1976) 2212-2214.
- [27] I. Petneházy, Z.M. Jászay, L. Tóke, Mechanism of the reaction of trialkyl phosphites with chalcones, Phosphorus, Sulfur, and Silicon and the Related Elements, 75 (1993) 103-106.
- [28] K. Mistry, M. Mehta, N. Mendpara, S. Gamit, G. Shah, Determination of antibacterial activity and MIC of crude extract of Abrus precatorius L, Adv Biotech, 10 (2010) 25-27.

- [29] O.C.U.a.N.E. . Antibacterial Activity of Abrus precatorius (Linn.) Leaf Extract Against Multi-resistant Wound Bacterial Isolates., Research Journal of Medicinal Plants, , 14 (I.020.) 88-95.
- [30] H.B. Küçük, A. Yusufoğlu, E. Mataracı, S. Döşler, Synthesis and biological activity of new 1, 3-dioxolanes as potential antibacterial and antifungal compounds, Molecules, 16 (2011) 6806-6815.
- [31] K. Iwasa, M. Kamigauchi, M. Ueki, M. Taniguchi, Antibacterial activity and structure-activity relationships of berberine analogs, European journal of medicinal chemistry, 31 (1996) 469-478.
- [32] M.E. Badawy, Structure and antimicrobial activity relationship of quaternary N-alkyl chitosan derivatives against some plant pathogens, Journal of Applied Polymer Science, 117 (2010) 960-969.
- [33] W. Sajomsang, P. Gonil, S. Saesoo, C. Ovatlarnporn, Antifungal property of quaternized chitosan and its derivatives, International journal of biological macromolecules, 50 (2012) 263-269.
- [34] S. Malladi, R.V. Nadh, K.S. Babu, P.S. Babu, Synthesis and antibacterial activity studies of 2, 4-di substituted furan derivatives, Beni-Suef University journal of basic and applied sciences, 6 (2017) 345-353.
- [35] S. Ravikumar, M.S. Ali, A. Ramu, M. Ferosekhan, Antibacterial activity of chosen mangrove plants against bacterial specified pathogens, World Applied Sciences Journal, 14 (2011) 1198-1202.
- [36] E. Al-Masri, M. Al-Refai, H.T. Al-Masri, B.F. Ali, S. Makhseed, L. Salah, B. Ghazal, A. Geyer, S.I. Ivlev, M. Abu-Sini, Synthesis, characterization, crystal structure, and fluorescence behavior of new 4-aryl-6-(2,5-dichlorothiophen-3-yl)-2-methylpyridine-3-carbonitrile derivatives, Journal of Molecular Structure, 1271 (2023) 134034.
- [37] R. Mishra, A. Srivastava, A. Sharma, P. Tandon, C. Baraldi, M.C. Gamberini, Structural, electronic, thermodynamical and charge transfer properties of Chloramphenicol Palmitate using vibrational spectroscopy and DFT calculations, Spectrochimica Acta Part A: Molecular and Biomolecular Spectroscopy, 101 (2013) 335-342.
- [38] H. K'Tir, A. Amira, C. Benzaid, Z. Aouf, S. Benharoun, Y. Chemam, R. Zerrouki, N.-E. Aouf, Synthesis, bioinformatics and biological evaluation of novel  $\alpha$ -aminophosphonates as antibacterial agents: DFT, molecular docking and ADME/T studies, Journal of Molecular Structure, 1250 (2022) 131635.
- [39] R. Then, Dihydropteroate Synthase\*, in: S.J. Enna, D.B. Bylund (Eds.) xPharm: The Comprehensive Pharmacology Reference, Elsevier, New York, 2007, pp. 1-7.
- [40] D. Fernández-Villa, M.R. Aguilar, L. Rojo, Folic Acid Antagonists: Antimicrobial and Immunomodulating Mechanisms and Applications, Int J Mol Sci, 20 (2019).
- [41] M. Venkatesan, M. Fruci, L.A. Verellen, T. Skarina, N. Mesa, R. Flick, C. Pham, R. Mahadevan, P.J. Stogios, A. Savchenko, Molecular mechanism of plasmid-borne resistance to sulfonamide antibiotics, Nature Communications, 14 (2023) 4031.
- [42] R.A. Azzam, R.E. Elsayed, G.H. Elgemeie, Design, Synthesis, and Antimicrobial Evaluation of a New Series of N-Sulfonamide 2-Pyridones as Dual Inhibitors of DHPS and DHFR Enzymes, ACS Omega, 5 (2020) 10401-10414.
- [43] Y. Zhao, W.R. Shadrick, M.J. Wallace, Y. Wu, E.C. Griffith, J. Qi, M.-K. Yun, S.W. White, R.E. Lee, Pterin–sulfa conjugates as dihydropteroate synthase inhibitors and antibacterial agents, Bioorganic & Medicinal Chemistry Letters, 26 (2016) 3950-3954.
- [44] R. Bahadi, M. Berredjem, C. Benzaid, F. Bouchareb, A. Dekir, M.L. Djendi, M. Ibrahim-Ouali, M. Boussaker, S. Bouacida, A.R. Bhat, S. Ahmed, K. Bachari, R. Redjemia, Efficient synthesis, crystallography study, antibacterial/antifungal activities, DFT/ADMET studies and molecular docking of novel α-aminophosphonates, Journal of Molecular Structure, 1289 (2023) 135849.
- [45] M.J. Frisch, G.W. Trucks, H.B. Schlegel, G.E. Scuseria, M.A. Robb, J.R. Cheeseman, G. Scalmani, V. Barone, G.A. Petersson, H. Nakatsuji, X. Li, M. Caricato, A.V. Marenich, J. Bloino, B.G. Janesko, R. Gomperts, B. Mennucci, H.P. Hratchian, J.V. Ortiz, A.F. Izmaylov, J.L. Sonnenberg, Williams, F. Ding, F. Lipparini, F. Egidi, J. Goings, B. Peng, A. Petrone, T. Henderson, D. Ranasinghe, V.G. Zakrzewski, J. Gao, N. Rega, G. Zheng, W. Liang, M. Hada, M. Ehara, K. Toyota, R. Fukuda, J. Hasegawa, M. Ishida, T. Nakajima, Y. Honda, O. Kitao, H. Nakai, T. Vreven, K. Throssell, J.A. Montgomery Jr., J.E. Peralta, F. Ogliaro, M.J. Bearpark, J.J. Heyd, E.N. Brothers, K.N. Kudin, V.N. Staroverov, T.A. Keith, R. Kobayashi, J. Normand, K. Raghavachari, A.P. Rendell, J.C. Burant, S.S. Iyengar, J. Tomasi, M. Cossi, J.M. Millam, M. Klene, C. Adamo, R. Cammi, J.W. Ochterski, R.L. Martin, K. Morokuma, O. Farkas, J.B. Foresman, D.J. Fox, Gaussian 16 Rev. C.01, Wallingford, CT 2016
- [46] M.P. Andersson, P. Uvdal, New Scale Factors for Harmonic Vibrational Frequencies Using the B3LYP Density Functional Method with the Triple- $\zeta$  Basis Set 6-311+G(d,p), The Journal of Physical Chemistry A, 109 (2005) 2937-2941.

- [47] A.R. Bhat, R.S. Dongre, F.A. Almalki, M. Berredjem, M. Aissaoui, R. Touzani, T.B. Hadda, M.S. Akhter, Synthesis, biological activity and POM/DFT/docking analyses of annulated pyrano[2,3-d]pyrimidine derivatives: Identification of antibacterial and antitumor pharmacophore sites, Bioorganic Chemistry, 106 (2021) 104480.
- [48] M. Guerfi, M. Berredjem, R. Bahadi, S.-E. Djouad, A. Bouzina, M. Aissaoui, An efficient synthesis, characterization, DFT study and molecular docking of novel sulfonylcycloureas, Journal of Molecular Structure, 1236 (2021) 130327.
- [49] P.E. Hartnett, C.M. Mauck, M.A. Harris, R.M. Young, Y.-L. Wu, T.J. Marks, M.R. Wasielewski, Influence of Anion Delocalization on Electron Transfer in a Covalent Porphyrin Donor–Perylenediimide Dimer Acceptor System, Journal of the American Chemical Society, 139 (2017) 749-756.
- [50] H. Xu, D.C. Xu, Y. Wang, Natural Indices for the Chemical Hardness/Softness of Metal Cations and Ligands, ACS Omega, 2 (2017) 7185-7193.
- [51] M.M. Makhlouf, A.S. Radwan, B. Ghazal, Experimental and DFT insights into molecular structure and optical properties of new chalcones as promising photosensitizers towards solar cell applications, Applied Surface Science, 452 (2018) 337-351.
- [52] H. Tavakol, H. Haghshenas, A DFT Study on the Interaction of Doped Carbon Nanotubes with H2S, SO2 and Thiophene, Quantum Reports, 3 (2021) 366-375.
- [53] M. Yoosefian, E. Rahmanifar, N. Etminan, Nanocarrier for levodopa Parkinson therapeutic drug; comprehensive benserazide analysis, Artif Cells Nanomed Biotechnol, 46 (2018) 434-446.